

1 **TO REFEREE #3**

2 Thank you very much for all your suggestions and comments. Next, we respond all your
3 suggestions in order.

4 1. The core (as the objective states) of the work is characterizing NDVI distribution
5 functions; the introduction should also include a review of different works done on
6 this, no matter for what application this was done, and what functions better
7 succeed in reproducing the statistical behaviour of this variable on different time
8 scales.

9 We present this study as a novelty of NDVI time characterization without Normal
10 assumption. In the introduction we have explained NDVI characterization when it
11 is used in the index-based insurance context, and assuming normal distributions.

12 2. Additionally, the introduction should also refer to what limitations assuming the
13 normal distribution has for NDVI characterization.

14 We have dealt with this topic in the result section because limitations assuming
15 the normal distribution are part of our results and conclusions. Different NDVI
16 distribution assumptions involve different damaged NDVI thresholds.

17 3. This being said, I think the objective should be more specific. On what time and
18 spatial scales NDVI is defined for the work to be done? The variable should be very
19 precisely defined.

20 This study uses information of MODIS with some limitations in time and scale. In
21 the “Material and methods” section we explain that product MOD09A1 has a
22 spatial resolution of 500m x 500m and a time resolution of 8 days. In future
23 researches we would like to prove with more spatial and time resolution using
24 other products. Any case, we think we would obtain the same essential conclusion:
25 Normal characterization is not the best in some intervals (mainly in spring and
26 autumn).

27 4. I wonder how representative the presented study case is for the generalization of
28 the results and conclusion. Different decisions made to develop this work should
29 be justified: crop to evaluate, location, number of pixels, sensor... Why only some
30 pixels and not the whole crop area?

31 We have analyzed pasture in this study because this kind of crop uses NDVI
32 characterization to define damage thresholds in the context of satellite index-base
33 insurances. The selected location is an example of pasture area without trees
34 dedicated to cattle breeding. You are right, this location is not very large and the
35 spatial resolution of the MODIS product is low, so we were limited to use not much
36 pixels. In future studies we want to select other more extensive pasture areas with
37 more resolution for obtaining more relevant results.

- 38 5. The choice of the candidate functions (see Table 3) must also be justified.
39 We have chosen these candidates because they are very common within
40 asymmetrical distribution and we have shown in this study that observed NDVI
41 distributions are essentially asymmetrical in many intervals (mainly in spring and
42 autumn). We could have used other candidates, but we think the conclusion would
43 be the same: normal assumption is not the best, and we recommend the use of
44 quantiles.
- 45 6. Lines 441-444. This assertion is highly dependent on how representative the
46 studied sample is of the case referred to, and to the general problem the paper
47 wants to address.
48 We have modified the paragraph eliminating the specific reference and talking
49 about the Normal assumption methodology in general. Now you can read:
50 "Therefore, the methodology using the NDVI Normal assumption applied to design
51 an index-based insurance will not be feasible in many intervals of this study."
- 52 7. From the figures in the Annex it is not so clear that GEV has an overall better
53 performance than the normal choice. In fact, in different examples both perform
54 very similarly.
55 You are right, GEV distributions fit better in spring and autumn intervals due to
56 distributions are mainly asymmetric in these periods. We have included a new
57 paragraph explaining this feature: Now you can read: "There is a relationship
58 between seasons and the number of intervals that fit correctly. We found that GEV
59 distributions explain better some intervals of spring and autumn since their
60 observed distributions are very asymmetric. On the other hand, we did not find an
61 important difference in winter, since its observed distributions are mainly
62 symmetric".
- 63 8. I was expecting to find in the results more depth regarding the impact that a
64 different distribution has on the parts (insurance companies and clients). At the
65 end, even if statistically another function performs better than the normal
66 assumption, the relevant issue is how much the benefit/loss is changed by this. A
67 better performance might have only a minor impact on the final result in the
68 insurance context. At least some estimation should be included.
69 In this study we have focused in the statistical analysis and how the thresholds
70 would be affected by the use of GEV assumption instead of the Normal one. We
71 have also offered some estimation about the probability of being below the NDVI
72 threshold in both assumptions. The probability obtained by GEV distributions is
73 mostly lower than the Normal distributions in spring, autumn and winter, that is
74 the working period of the insurance. In future works we will be able to focus in
75 more economical aspects and to perform some simulation of the overall process.

- 76 9. Additionally, no discussion is done on other works in the results regarding the
77 insurance context.
78 In this study we have shown up the differences in using Normal and GEV
79 distributions in the insurance context. Differences in the probability of being below
80 the NDVI threshold recommend us the use of quantiles instead of preset
81 distributions.
- 82 10. Please, check that captions of tables and figures are self-explanatory (see for
83 instance Table1; provide study period).
84 We have included the study period in the caption of table 1.
- 85 11. The weather variables statistics included in Table 1 just presents the local climate.
86 Is it possible to combine this information with the NDVI monitoring to obtain
87 better indexes or to validate the NDVI results?
88 Some studies have dealt with the combination of weather variables and NDVI to
89 create a better index, however in this study we have focused in the statistical
90 analysis of NDVI distributions without questioning whether NDVI is the best index
91 or not.
- 92 12. Line 246. "... the completed station of meteorological networks". What do you
93 mean by that?
94 We made a mistake with the translation. A completed station means a main or
95 principal station with the majority of weather measure equipments.
- 96 13. Lines 306-311. What is the purpose of the last sentence?
97 We have not found the use of this HSL criterion in the context of NDVI remote
98 sensing images. Therefore it can be considered a novelty method to eliminate
99 wrong values in a NDVI series.
- 100 14. Line 367. Please, define this more precisely.
101 This entire paragraph has been rewritten to clarify all the definitions presented on
102 it.
- 103 15. Line 371. I think the definition of VR can be more clearly expressed. Additionally,
104 the use of tables for VR intervals results in too long and repeated content.
105 This entire paragraph has been rewritten to clarify all the definitions presented on
106 it, and table 3 has been simplified.
- 107 16. Contents in lines 367-376 and 415-432 should be moved to the Methods sections.
108 We think some of these paragraphs could stay at the result section due to they are
109 applications of the methodology presented in the Method section (MLM and Chi
110 square test). We attend some of your suggestions and move the paragraph
111 regarding to PDF candidates to the Method section.
- 112 17. Line 451. I would suggest not to use the future tense here.
113 We have modified from future tense to past tense.

114 18. Please, check the references' format meets the Journal's standards.

115 [We have reviewed the format references.](#)

116

117

Statistical Analysis for Satellite Index-Based Insurance to define Damaged Pasture Thresholds

Juan José Martín-Sotoca^{1*}, Antonio Saa-Requejo^{2,3}, Rubén Moratíel^{2,3}, Nicolas Dalezios⁴, Ioannis Faraslis⁵, and Ana María Tarquis^{2,6}

jmartinsotoca@gmail.com, antonio.saa@upm.es, ruben.moratíel@upm.es, dalezios.n.r@gmail.com, faraslisgiannis@yahoo.gr, anamaria.tarquis@upm.es

¹ Data Science Laboratory. European University, Madrid, Spain.

² CEIGRAM, Research Centre for the Management of Agricultural and Environmental Risks, Madrid, Spain.

³ Dpto. Producción Agraria. Universidad Politécnica de Madrid, Spain.

⁴ Department of Civil Engineering. University of Thessaly, Volos, Greece.

⁵ Department of Planning and Regional Development. University of Thessaly, Volos, Greece.

⁶ Grupo de Sistemas Complejos. Universidad Politécnica de Madrid, Spain.

* Correspondence to: jmartinsotoca@gmail.com

Abstract: Vegetation indices based on satellite images, such as Normalized Difference Vegetation Index (NDVI), have been used in countries like USA, Canada and Spain for damaged pasture and forage insurance for the last years. This type of agricultural insurance is called “satellite index-based insurance” (SIBI). In SIBI, the occurrence of damage is defined through NDVI thresholds mainly based on statistics derived from Normal distributions. In this work a pasture area at the north of Community of Madrid (Spain) has been delimited by means of **Moderate Resolution Imaging Spectroradiometer** (MODIS) images. A statistical analysis of NDVI histograms was applied to seek for the best statistical distribution using maximum likelihood method. The results show that the Normal distribution is not the optimal representation and the General Extreme Value (GEV) distribution presents a better fit through the year. A comparison between Normal and GEV are showed respect to the probability under a NDVI threshold value along the year. This suggests that a priori distribution should not be selected and a percentile methodology should be used to define a NDVI damage threshold rather than the average and standard deviation, typically of Normal distributions.

Keywords: NDVI, pasture insurance, GEV distribution, MODIS.

Highlights

- **General Extreme Value (GEV) distribution provides the best fit to the NDVI historical observations.**
- **Difference between Normal and GEV distributions are higher during spring and autumn, transition periods in the precipitation regimen.**
- **NDVI damage threshold shows evident differences using Normal and GEV distributions covering both the same probability (24.20%).**

- 156 • **NDVI damage threshold values based on percentiles calculation is proposed as an**
157 **improvement in the index based insurance in damaged pasture.**

158

159 **1. Introduction**

160 Agricultural insurance addresses the reduction of the risk associated with crop
161 production and animal husbandry. The concept of index-based insurance (IBI) attempts to
162 achieve settlements based on the value taken by an objective index rather than on a case-
163 by-case assessment of crop or livestock losses (Gommes and Kayitakier, 2013). Indeed, the
164 goal of IBI policy remains to develop an affordable tool to all producers, including
165 smallholders. Specifically, IBI can constitute a safety net against weather-related risks for
166 all members of the farming community, thereby increasing food security and reducing the
167 vulnerability of rural populations to weather extremes. Moreover, IBI can be associated
168 with credits for insured smallholders, due to the fact that the risk of non-repayment for
169 lenders is reduced, which encourages the use of agricultural inputs and equipment,
170 leading to increased and more stable crop production. Over the past decade, the
171 importance of weather index-based insurances (WIBI) for agriculture has been increasing,
172 mainly in developing countries (Gommes and Kayitakier, 2013). This interest can be
173 explained by the potential that IBI constitutes a risk management instrument for small
174 farmers. Indeed, it can be considered within the context of renewed attention to
175 agricultural development as one of the milestones of poverty reduction and increased
176 food security, as well as the accompanying efforts from various stakeholders to develop
177 agricultural risk management instruments, including agricultural insurance products.

178

179 Farmers need to protect their land and crops specifically from drought in arid and
180 semi-arid countries, since their production may directly depend mainly on the impacts of
181 this particular natural hazard. Insurance for drought-damaged lands and crops is currently
182 the main instrument and tool that farmers can resort in order to deal with agricultural
183 production losses due to drought. Many of these insurances are using satellite vegetation
184 indices (Rao, 2010), thus they are also called “satellite index-based insurances” (SIBI). SIBI
185 have some advantages over WIBI, such as cost-effective information and acceptable
186 spatial and temporal resolution. They do not, however, resolve the issue of basis risk, i.e.
187 potential unfairness to insurance takers (Leblois, 2012). Moreover, the very nature of an
188 index-based product creates the chance that an insured party may not be paid when they
189 suffer loss. For this reason, in some countries (Spain) they have named this SIBI as
190 “damaged in pasture” to cover not only drought even this one is the main cause.

191

192 It is highly recognized that shortage of water has many implications to agriculture,
193 society, economy and ecosystems. Specifically, its impact on water supply, crop
194 production and rearing of livestock is substantial in agriculture. Knowing the likelihood of
195 drought is essential for impact prevention (Dalezios, 2013). Drought severity assessment
196 can be approached in different ways: through conventional indices based on
197 meteorological data, such as temperature, rainfall, moisture, etc. (Niemeyer, 2008), as
198 well as through remote sensing indices based on images usually taken by artificial
199 satellites (Lovejoy et al., 2008) or drones. In the second group they are found Satellite
200 Vegetation Indices (SVI), which can quantify “green vegetation”, and soil moisture through
201 Soil Water Index (Gouveia et al., 2009) combining different spectral reflectances. Thus,
202 they are one of the main ways to quantitatively assess drought severity.

203

204 At the present time, several satellites (NOAA, TERRA, DEIMOS, etc.) can provide this
205 spectral information with different spatial resolution. Some series with a high temporal
206 frequency are freely available, those from NOAA satellites and Terra. The most widely
207 known SVI is the Normalized Difference Vegetation Index (NDVI). It follows the principle
208 that healthy vegetation mainly reflects the near-infrared frequency band. There are
209 several other important SVI, such as Soil Adjusted Vegetation Index (SAVI) and Enhanced
210 Vegetation Index (EVI) that incorporate soil effects and atmospheric impacts, respectively.
211 An important point of this class of insurance is “when damage occurs”. To measure this, a
212 SVI threshold value is defined mainly based on statistics that apply to Normal distributed
213 variables: average and standard deviation. When current SVI values are below this
214 threshold value for a period of time, insurance recognizes that a damage is occurring,
215 most of the times drought, and then it begins to pay compensations to farmers.

216

217 WIBI aims to protect farmers against weather-based disasters such as droughts, frosts
218 and floods. A WIBI policy links possible insurance payouts with the weather requirements
219 of the crop being insured: the insurer pays an indemnity whenever the realized value of
220 the weather index meets a specified threshold. Whereas payouts in traditional insurance
221 programs are related to actual crop damages, a farmer insured under a WIBI contract may
222 receive a payout. A current difficulty to the wide implementation of WIBI is the weakness
223 of indices. Indeed, there is certainly a need for more efficient indices based on the
224 additional experience gained from the implementation of WIBI products in the developing
225 world. Current trends in index technology are exciting and they actuate high expectations,
226 especially the development of yield indices and the use of remote sensing inputs. Risk
227 protection and insurance illiteracy constitute another difficulty, which has to be addressed
228 by training and awareness-raising at all levels, from farmers to farmers’ associations,
229 micro-insurance partners, as well as senior decision-makers in insurance, banking, and

230 politics (Bailey, 2013). It is essential that all stakeholders (especially the insured) perfectly
231 understand the principles of IBI, as otherwise the insurer, even the whole concept of
232 insurance, is at risk of reputation loss for years or decades.

233

234 There is currently a lack of technical capacity in the insurance sectors of most
235 developing countries, which is a constraint to the scaling up and further development of
236 WIBI (Gommes and Kayitakire, 2012). Specifically, although it is possible to design an index
237 product and assist in roll-out, marketing, and sales, such assistance is not possible on a
238 wide scale, simply because there is lack of qualified expertise. Indeed, it usually requires
239 mathematical modeling, data manipulation, and expertise in crop simulation to design an
240 index. Nevertheless, it is possible to structure insurance with multiple indices, but this
241 increases the complexity of the product and makes it difficult for farmers to comprehend
242 it. ‘Basis risk’ is also a particular problem for index products, which is frequently caused by
243 the fact that measurements of a particular variable, such as rain, may differ at the
244 insurer’s measurement site and in the farmer’s field. This also creates problems for
245 insurance providers. Indeed, part of the reason the scaling up of index products has failed
246 is that both insurers and farmers suffer from this basis risk.

247

248 Currently, to mitigate impacts of climate-related reduced productivity of French
249 grasslands, several studies have been developed to design new insurance scheme bases
250 indemnity payouts to farmers on a forage production index (FPI) (Rumiguié et al., 2015;
251 2017). Two examples of SIBIs are presented in two different countries: USA and Spain. In
252 particular, in USA there are several insurance programs for pasture, rangeland and forage,
253 which use various indexing systems (rainfall and vegetation indices), and are promoted by
254 Unites States Department of Agriculture (USDA) (Maples et al., 2016; USDA, 2018). NDVI is
255 the index chosen in the vegetation index program and it is obtained from AVHRR
256 (Advanced Very High Resolution Radiometer) sensor onboard NOAA satellites. Average,
257 maximum and minimum NDVI values are obtained from a historical series with the aim of
258 calculating a trigger value. Insurer decides the quantity of compensation comparing this
259 trigger with current value. On the other hand, in Spain there exists the “Insurance for
260 Damaged Pasture” from “Spanish System of Agricultural Insurance” (BOE, 2013). This
261 insurance defines damage event through NDVI values obtained from MODIS sensor
262 onboard TERRA satellite of NASA. In this insurance, NDVI threshold values ($NDVI_{th}$) are
263 calculated subtracting several times ($k = 0.7$ or $k = 1.5$) standard deviation to average
264 within a homogeneous area:

265

266

267

$$NDVI_{th} = \mu - k \cdot \sigma \quad (1)$$

268 where μ, σ are average and standard deviation of NDVI respectively. Average and standard
269 deviation come of supposing Normal distributions in the historical data (Goward et al.,
270 1985; Hobbs, 1995; Fuller, 1998; Al-Bakri and Taylor, 2003; Turvey et al., 2012; De Leeuw
271 et al. 2014).

272

273 The aim of this paper is to find a more realistic statistical NDVI distribution without
274 the “a priori” assumption that variables follow a Normal distribution, typically for current
275 SIBI methodology. In order to achieve this, the Maximum Likelihood Method (MLM) is
276 fitted to a historical series of NDVI values in a pasture land area in Spain (Community of
277 Madrid). Different types of asymmetrical distributions are examined with the aim to find a
278 better fit than Normal. To eliminate some noise in the historical series, an original method
279 is applied consisting of using Hue-Saturation-Lightness (HSL) color model. Finally, Chi-
280 square test (χ^2 test) has been used to check the goodness of fit for all considered
281 distributions.

282

283

284 **2. Materials and Methods**

285 **2.1 Vegetation Index**

286 The differences of the reflectance of green vegetation in parts of the electromagnetic
287 radiation spectrum, namely, visible and near infrared, provide an innovative method for
288 monitoring surface vegetation from space. Specifically, the spectral behavior of vegetation
289 cover in the visible (0.4-0.7mm) and near infrared (0.74-1.1mm, 1.3-2.5mm) offers the
290 possibility to monitor from space the changes in the different stages of cultivated and
291 uncultivated plants taking also into account the corresponding behavior of the
292 surrounding microenvironment (Ortega-Farias et al., 2016). Indeed, from the visible part
293 of the electromagnetic radiation spectrum it is possible to draw conclusions about the
294 rate photosynthesis, whereas from near infrared inferences are extracted about the
295 chlorophyll density and the amount of canopy in the plant mass, as well as the water
296 content in the leaves, which is also linked directly to the rate of transpiration with impacts
297 to physiological process of photosynthesis. Usually, data from NOAA/AVHRR series of
298 polar orbit meteorological satellites are used with low spatial resolution (1.1 km^2) and
299 recurrence interval at least twice daily from the same location. Several algorithms
300 combining channels of red (RED), near infrared (NIR) and green (GREEN) have been
301 proposed, which provide indices sensitive to green vegetation.

302

303 NDVI uses two frequency bands: red band (660 nm) and near-infrared band (860 nm).
304 Absorption of red band is related to photosynthetic activity and reflectance of near-
305 infrared band is related to presence of vegetation canopies (Flynn, 2006). In drought
306 periods, NDVI values can reduce significantly, therefore many researchers have used this
307 index to measure drought events in recent years (Dalezios et al., 2014). To calculate NDVI
308 we will use this mathematical formula:

$$310 \quad NDVI = \frac{IR-R}{IR+R} \quad (2)$$

311
312 where IR and R are reflectance values in Near-Infrared band and Red band, respectively.
313 NDVI values below zero indicate no photosynthetic activity and are characteristic of areas
314 with large accumulation of water, such as rivers, lakes, or reservoirs. The higher is the
315 NDVI value, the greater is the photosynthetic activity and vegetation canopies.

316
317 In this paper, the NDVI is used, which is widely known index with a multitude of
318 applications over time. The NDVI is suited for monitoring of total vegetation, since it partly
319 compensates the changes in light conditions, land slope and field of view (Kundu et al.,
320 2016). In addition, clouds, water and snow show higher reflectance in the visible than in
321 the near infrared, thus, they have negative NDVI values. Indeed, bare and rocky terrain
322 show vegetation index values close to zero. Moreover, the NDVI constitutes a measure of
323 the degree of absorption by chlorophyll in the red band of the electromagnetic spectrum.
324 In summary, the NDVI is a reliable index of the chlorophyll density on the leaves, as well as
325 the percentage of the leaf area density over land, thus, NDVI constitutes a credible
326 measure for the assessment of dry matter (biomass) in various species vegetation cover
327 (Dalezios, 2013). It is clear from the above that the NDVI is an index closely related to
328 growth and development of plants, which can effectively monitor surface vegetation from
329 space.

330
331 The continuous increase of the NDVI value during the growing season reflects the
332 vegetative and reproductive growth due to intense photosynthetic activity, as well as the
333 satisfactory correlation with the final biomass production at the end of a growing period.
334 On the other hand, gradual decrease of the NDVI values signifies stress due to lack of
335 water or extremely high temperatures for the plants, leading to a reduction of the
336 photosynthetic rate and ultimately a qualitative and quantitative degradation of plants.
337 NDVI values above zero indicate the existence of green vegetation (chlorophyll), or bare
338 soil (values around zero), whereas values below zero indicate the existence of water,
339 snow, ice and clouds.

340

341 **2.2 Database**

342 Scientific research satellite Terra (EOS AM-1) has been chosen to provide necessary
343 information to calculate NDVI in the study area. This satellite was launched into orbit by
344 NASA on December 18, 1999. MODIS sensor aboard this satellite collects information of
345 different reflectance bands. MODIS information is organized by "products". The product
346 used in this study was MOD09A1 (LP DAAC, 2014). MOD09A1 incorporates seven
347 frequency bands: Band 1 (620-670 nm), band 2 (841-876 nm), band 3 (459-479 nm), band
348 4 (545-565 nm), 5 band (1230-1250 nm), band 6 (1628-1652 nm) and band 7 (2105-2155
349 nm). The bands used to calculate NDVI are: band 1 for red frequency and band 2 for near-
350 infrared frequency. MOD09A1 provides georeferenced images with pixel resolution of
351 500m x 500m. This product has a mix of the best reflectance measures of each pixel in an
352 8-days period. The period of time selected on this study was from 2002 to 2017.

353

354 Daily data from a **principal station** of the meteorological network were utilized during
355 the period studied (2002 – 2017). Meteorological station is located in 40°41'46"N
356 3°45'54"W (elevation 1004 m a.s.l.), less than 2 km from the study area (AEMET, 2017).

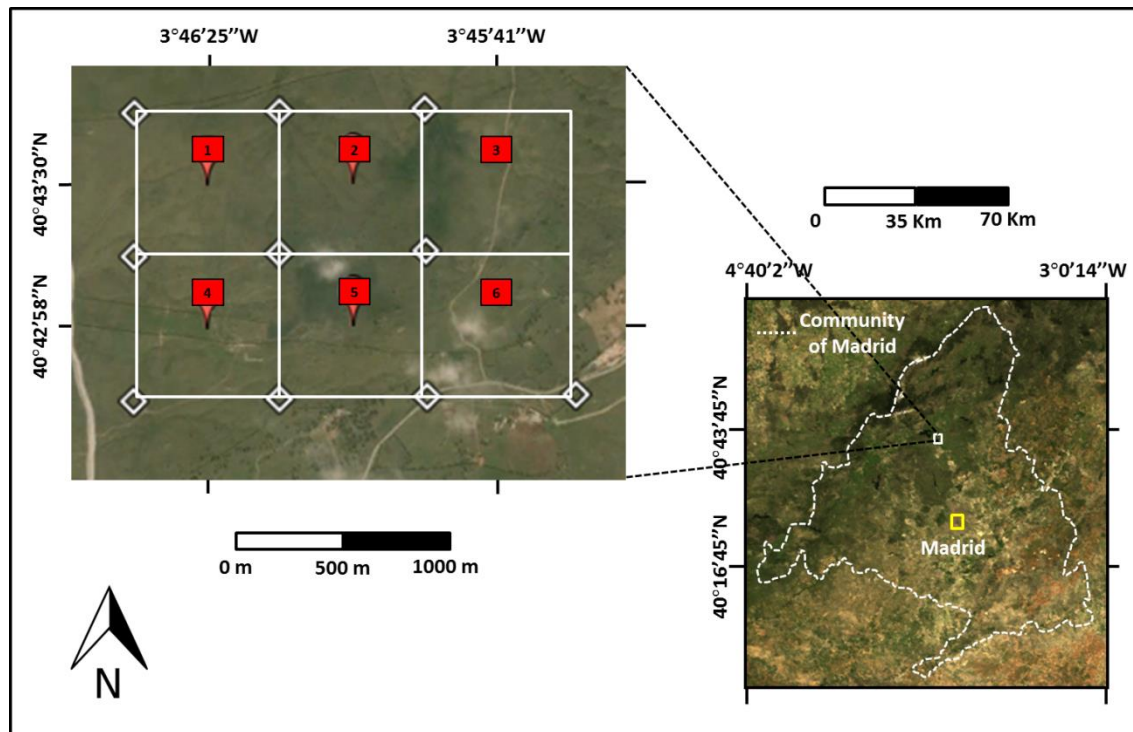
357

358 **2.3 Site description**

359 Six pixels (500m x 500m) are considered located in a pasture area at the north of the
360 Community of Madrid (Spain) between the municipalities of "Soto del Real" and
361 "Colmenar Viejo". The study area is located between meridians 3° 45' 00" and 3° 47' 00"
362 W and parallels 40° 42' 00" and 40° 44' 00" N approximately (see Fig. 1).

363

364



365

366

367

Figure 1. The study area is in the centre of the Iberian Peninsula (Community of Madrid). RGB image of six pixels area used for case study is shown (Google Earth's and MODIS images).

368

369

370

371

372

373

374

375

376

377

The annual mean temperature ranges during the study period from 12.7°C to 13.8°C, and annual mean precipitation ranges from 360 mm to 781 mm. The stations studied were identified semi-arid (annual ratio P/ET_o between 0.2 and 0.5) according to the global aridity index developed by the United-Nations Convention to Combat Desertification (UNEP, 1997). According to the climatic classification of Köppen (Kottek et al., 2006), this area presents a continental Mediterranean climate temperate with dry and temperate summer (type Csb). Temperature and precipitation of this site, based on 20 years, is presented in Table 1.

378

379

380

381

Due to high soil moisture conditions, ash is the dominant tree, forming large agroforestry systems ("dehesas") that are used for pasture. These are ecosystems with high biodiversity.

382

383

Table 1. Monthly average of maximum temperature (T_{max}), average temperature (T_{avg}), minimum temperature (T_{min}) and precipitation (P). **Study period from 1997 to 2017.**

| Month | Jan | Feb | Mar | Apr | May | Jun | Jul | Aug | Sep | Oct | Nov | Dec | Annual |
|-----------------------|-----|-----|------|------|------|------|------|------|------|------|------|-----|--------|
| T _{max} (°C) | 7.1 | 9.3 | 12.7 | 15.4 | 19.5 | 24.6 | 28.6 | 28.1 | 23.7 | 16.8 | 11.1 | 7.4 | 17.0 |
| T _{avg} (°C) | 3.6 | 4.8 | 7.7 | 10.1 | 13.7 | 18.4 | 22.0 | 21.7 | 17.9 | 12.3 | 7.1 | 4.1 | 12.0 |

| | | | | | | | | | | | | | |
|-----------|------|------|------|------|------|------|------|------|------|------|------|------|-------|
| Tmin (°C) | 0.0 | 0.3 | 2.6 | 4.8 | 7.8 | 12.1 | 15.4 | 15.3 | 12.0 | 7.8 | 3.0 | 0.8 | 6.8 |
| P (mm) | 67.2 | 50.0 | 38.5 | 62.2 | 62.3 | 30.2 | 18.9 | 16.4 | 34.2 | 79.3 | 86.2 | 82.6 | 627.9 |

384

385 **2.4 HSL model**

386 There is no doubt that NDVI time-series from satellite sensors carry useful
 387 information, which can be used for characterizing seasonal dynamics of vegetation
 388 (Fensholt et al., 2012; Forkel et al., 2013). However, due to unfavorable atmospheric
 389 conditions during the data acquisition, NDVI time-series curve often contains noise
 390 (Motohka et al., 2011; Park, 2013). Although most of the NDVI data products are
 391 temporally composited through maximum value compositing (MVC) method (Holben,
 392 1986) to retain relatively cloud-free data, residual noise still exists in the data, which will
 393 affect the accuracy of the NDVI value.

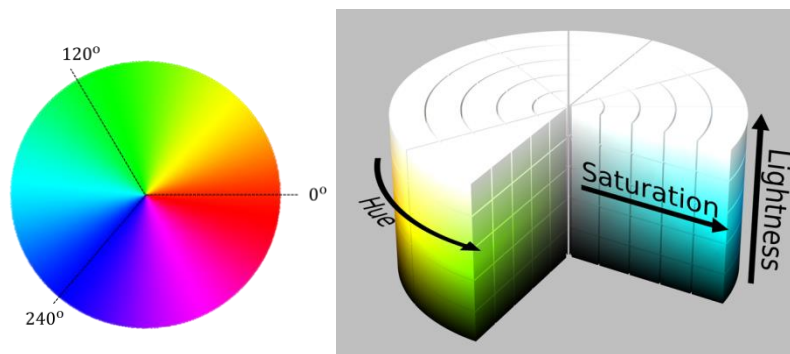
394

395 Therefore, usually it is necessary to reconstruct of NDVI time-series before extracting
 396 information from the noisy data. There are several techniques that have been applied to
 397 reduce noise and reconstruct NDVI series, a summary of these can be found in Wei et al.
 398 (2016). In this study we applied a simple filtering method based on the Hue-Saturation-
 399 Lightness (HSL) color model inspired by the work presented by Tackenberg (2007).

400

401 HSL color model is a cylindrical representation of RGB (Red-Green-Blue) points. Their
 402 components are Hue (color type), Saturation (level of color purity) and Lightness (color
 403 luminosity). Hue is the angular component and it is more intuitive for humans since it is
 404 directly related to the color wheel (see Fig. 2).

405



406

407 **Figure 2.** Colour wheel of Hue (on the left) and the HSL model (on the right).

408 Saturation is the radial component and near-zero values indicate grey colors.
 409 Lightness is the axial radial versus axial component, zero lightness produces black and full
 410 lightness produces white.

411

412 The NDVI series are filtered using the following HSL criterion: NDVI values are valid if
413 HSL Saturation is greater than 0.15. In this way, the values of the series that have grey
414 color correlate with pasture covered by clouds or snow are eliminated. This type of filter
415 based in HSL color space has been used on digital camera images monitoring vegetation
416 phenology (Tackenberg, 2007; Crimmins and Crimmins, 2008; Graham et al., 2009).
417 However, we have not found the use of this HSL criterion in the context of NDVI remote
418 sensing images.

419

420 **2.5 Maximum Likelihood Method (MLM)**

421 MLM estimates the set of parameters $\{\alpha, \beta, \mu, \sigma, \dots\}$ for a specific statistical
422 distribution that maximizes the “likelihood function” or the “joint density function”:

$$423 \quad L = f(\mathbf{x}, \boldsymbol{\theta}) = \prod_{i=1}^n f(x_i; \alpha, \beta, \mu, \sigma, \dots) \quad (3)$$

424 where $\mathbf{x} = (x_1, \dots, x_n)$ is the set of data, $\boldsymbol{\theta} = (\alpha, \beta, \mu, \sigma, \dots)$ is the vector of parameters
425 and $f(x_i; \alpha, \beta, \mu, \sigma, \dots)$ is the density function of the statistical model.

426 When maximization with respect to the vector of parameters is carried out, the
427 estimated parameters $(\hat{\alpha}, \hat{\beta}, \hat{\mu}, \hat{\sigma}, \dots)$ for the proposed statistical distribution are obtained
428 (Larson, 1982). Properties of estimated parameters are: invariance, consistency and
429 asymptotically unbiased.

430 In the case of a Gaussian model, the estimated statistics μ and σ are defined by
431 accurate expressions as follows:

$$432 \quad \hat{\mu} = \bar{x} = \frac{1}{n} \sum_{i=1}^n x_i \quad \hat{\sigma} = s = \sqrt{\frac{1}{n} \sum_{i=1}^n (x_i - \bar{x})^2} \quad (4)$$

433 where $\hat{\mu}$ is the sample mean and $\hat{\sigma}$ is the sample standard deviation of the data set.

434 In this study we will apply MLM to estimate the parameters for 4 probability density
435 functions (PDF). In Table 2, a brief description is presented of these PDF candidates:
436 Normal, Gamma, Beta and GEV. To do so, the following MATLAB functions have been
437 used: “normfit”, “gamfit”, “betafit” and “gevfit” (respectively).
438

439

Table 2. Candidate Probability Density Functions (PDF).

| PDF NAME | PDF EXPRESSION | PDF PARAMETERS |
|----------|----------------|----------------|
|----------|----------------|----------------|

| | | |
|--------|---|--|
| Normal | $f(x; \mu, \sigma) = \frac{1}{\sigma\sqrt{2\pi}} e^{-\frac{1}{2}\left(\frac{x-\mu}{\sigma}\right)^2}$ | $\mu \equiv \text{average}$ $\sigma \equiv \text{standard deviation}$ |
| Gamma | $f(x; \alpha, \beta) = \frac{1}{\beta^\alpha \Gamma(\alpha)} x^{\alpha-1} e^{-\frac{x}{\beta}}$ | $\Gamma(\cdot) \equiv \text{gamma function}$ $\alpha \text{ and } \beta \equiv \text{parameters}$ |
| Beta | $f(x; a, b) = \frac{\Gamma(a+b)}{\Gamma(a)\Gamma(b)} x^{a-1} (1-x)^{b-1}$ | $\Gamma(\cdot) \equiv \text{gamma function}$ $a \text{ and } b \equiv \text{parameters}$ |
| GEV | $f(x; \mu, \sigma, \xi) = \frac{1}{\sigma} t(x)^{\xi+1} e^{-t(x)}$ where $t(x) = \begin{cases} \left(1 + \left(\frac{x-\mu}{\sigma}\right)\xi\right)^{-1/\xi} & \text{if } \xi \neq 0 \\ e^{-(x-\mu)/\sigma} & \text{if } \xi = 0 \end{cases}$ | $\mu \in \mathbb{R} \equiv \text{location param.}$ $\sigma > 0 \equiv \text{scale parameter}$ $\xi \in \mathbb{R} \equiv \text{shape parameter}$ |

440

441

442 2.6 Goodness of fit (Chi-square test)

443 χ^2 test can be used to determine to what extent observed frequencies differ from
444 frequencies expected for a specific statistical model. The most important points of the
445 theory are briefly presented in (Cochran, 1952).

446 Let $f(x, \theta)$ be a theoretical density function of a random variable X which depends on
447 parameters $\theta = (\alpha, \beta, \mu, \sigma, \dots)$ and let x_1, \dots, x_n be a sample of X grouped into k classes with n_i
448 data per class i .

449 Firstly, the following hypothesis is set:

450 (H_0) observed data fit theoretical distribution $f(x, \theta)$.

451 Then the test statistic χ_c^2 is defined as:

$$452 \quad \chi_c^2 = \sum_{i=0}^k \frac{(n_i - e_i)^2}{e_i} \quad (5)$$

453 where n_i is the number of data or observed frequency and $e_i = n \cdot P(\text{class } i)$ is the
454 expected frequency for class i . $P(\text{class } i)$ is the theoretical interval probability defined for
455 class i .

456 A level of significance is also set as:

$$457 \quad \alpha = P(\text{Reject } H_0 / H_0 \text{ is true}) \quad (6)$$

458 Finally, the following decision rule is applied: "reject the theoretical distribution at
459 significance level α if:

$$460 \quad \chi_c^2 > \chi_{(k-m-1, 1-\alpha)}^2 \quad (7)$$

461 where $\chi^2_{(k-m-1, 1-\alpha)}$ is a χ^2 distribution with $k-m-1$ degrees of freedom (m is the number of
462 parameters, k is the number of classes).

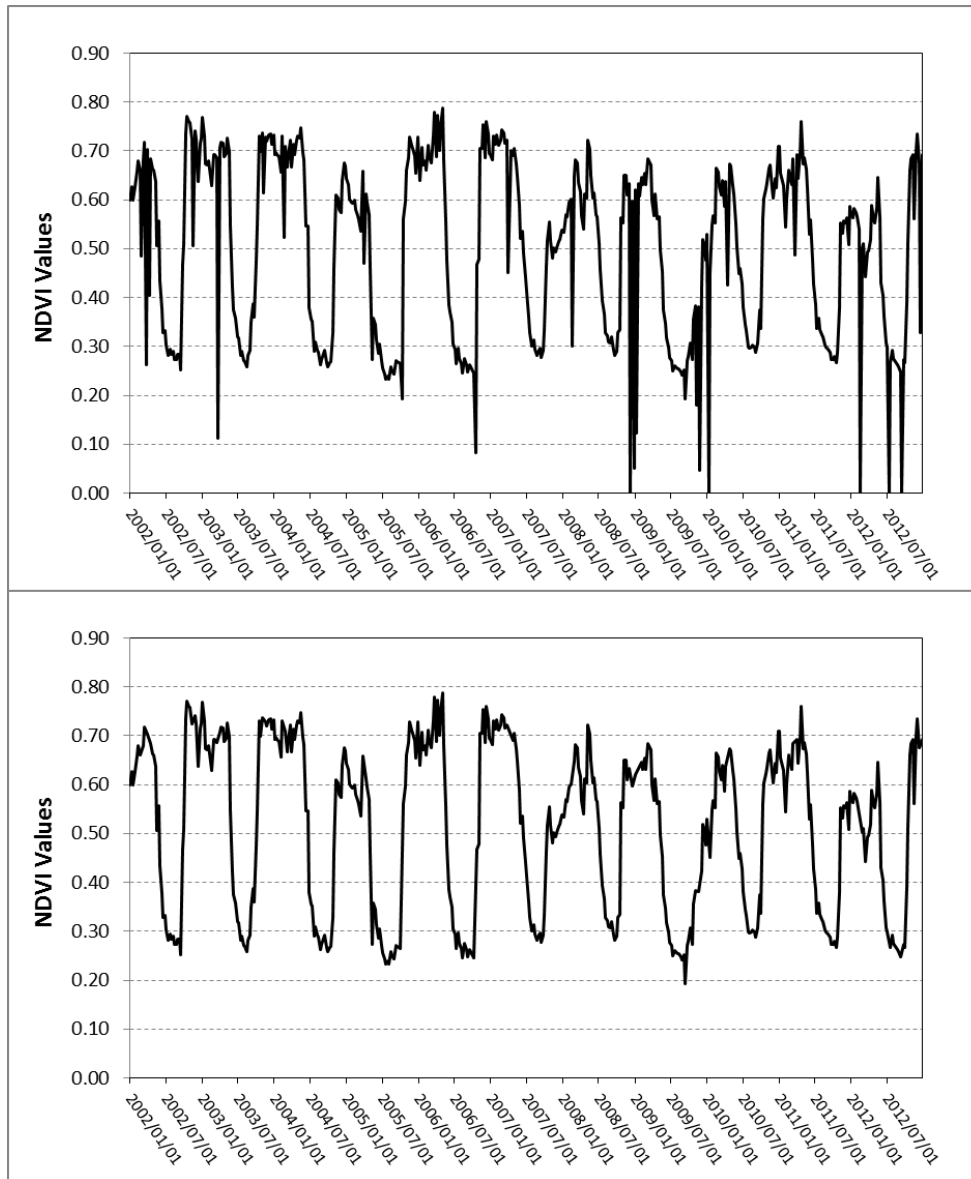
463

464

465 **3. Results and Discussion**

466 ***3.1 HSL filtering criterion***

467 NDVI series (from 2002 to 2017) were obtained for each pixel of the study area using
468 frequency bands provided by MODIS product named MOD09A1. These series contain
469 some irregular values that can skew NDVI pattern. Therefore, the six series (six pixels)
470 were filtered using the HSL criterion. **In Fig. 3 is shown an example of how HSL filtering
471 criterion works with a 10 years NDVI series (from 2002 to 2012).**



472

473 **Figure 3.** HSL filtering criterion applied to a 10 years NDVI series. Top graph shows the real NDVI
 474 series. Bottom graph shows the HSL filtered NDVI series.

475 The abrupt changes in the NDVI values, mainly observed during raining seasons such
 476 as autumn and winter, are efficiently eliminated. Not to be a high computational
 477 demanding method is one of the main advantages of HSL filtering method. Therefore, this
 478 method will allow us to obtain more robust NDVI values to be used in the statistical
 479 analysis.

480

481 **3.2 Maximum Likelihood Method (MLM) and Chi square test**

482 NDVI values were obtained consecutively every 8 days from MODIS product starting
 483 at 1st of January of every year, in such a way that 46 NDVI observations were considered
 484 for each year. Therefore, 46 Random Variables (RV) were defined when taking into
 485 account all the years of this study.

486 In Table 3, every RV (named as “Interval”) can be seen together with the number of
 487 available NDVI observations. Each RV collects the observations coming from the six
 488 selected pixels. The start intervals of each season are: interval 45 for winter, interval 11
 489 for spring, interval 23 for summer and interval 34 for autumn.

490

491

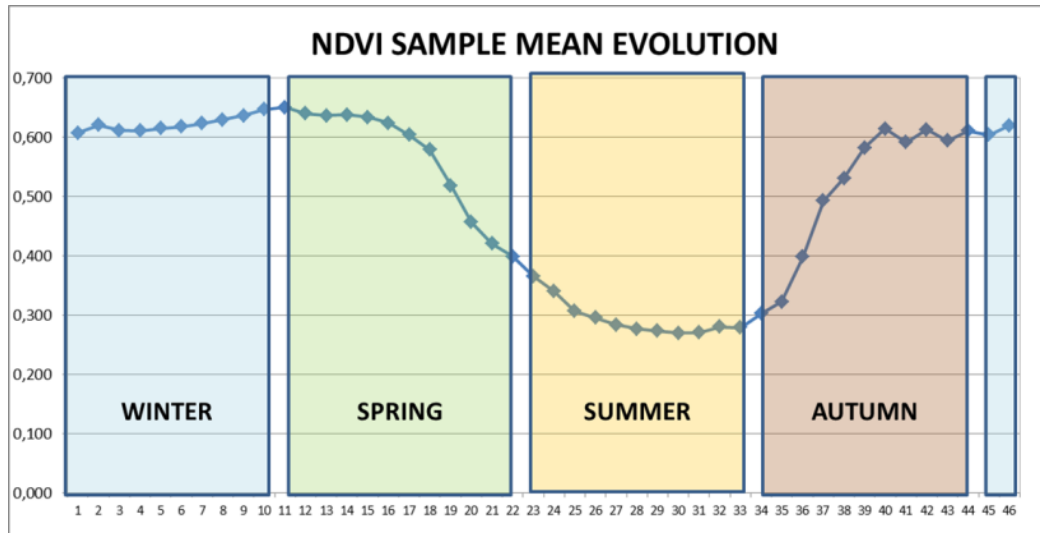
Table 3. Number of observations for every RV (named as Interval).

| RANDOM VARIABLE | # OBSERVATIONS | RANDOM VARIABLE | # OBSERVATIONS |
|-----------------|----------------|-----------------|----------------|
| Interval 1 | 85 | Interval 24 | 96 |
| Interval 2 | 84 | Interval 25 | 96 |
| Interval 3 | 96 | Interval 26 | 96 |
| Interval 4 | 96 | Interval 27 | 96 |
| Interval 5 | 95 | Interval 28 | 96 |
| Interval 6 | 90 | Interval 29 | 96 |
| Interval 7 | 86 | Interval 30 | 96 |
| Interval 8 | 83 | Interval 31 | 96 |
| Interval 9 | 96 | Interval 32 | 96 |
| Interval 10 | 96 | Interval 33 | 94 |
| Interval 11 | 74 | Interval 34 | 96 |
| Interval 12 | 88 | Interval 35 | 96 |
| Interval 13 | 88 | Interval 36 | 85 |
| Interval 14 | 88 | Interval 37 | 90 |
| Interval 15 | 96 | Interval 38 | 96 |
| Interval 16 | 92 | Interval 39 | 92 |
| Interval 17 | 88 | Interval 40 | 90 |
| Interval 18 | 96 | Interval 41 | 96 |
| Interval 19 | 95 | Interval 42 | 89 |
| Interval 20 | 96 | Interval 43 | 95 |
| Interval 21 | 95 | Interval 44 | 88 |
| Interval 22 | 96 | Interval 45 | 90 |
| Interval 23 | 96 | Interval 46 | 90 |

492

493

494 In Fig. 4, a plot with NDVI sample means of all RV with a start and end reference of the
495 astronomical seasons is shown. The typical evolution of the NDVI along a year can be
496 seen.
497



498 **Figure 4.** NDVI sample means of 46 random variables (RV) are shown as well as start and end
499 reference of every season. Study period from 2002 to 2017.
500

501
502 The observed evolution of NDVI through the different seasons is typical of the pasture
503 in this area. The summer presents the lowest mean values which begin to increase in
504 autumn achieving a maximum mean value of 0.60 or 0.65 during winter. In the middle of
505 the spring NDVI decrease again, approaching the lowest mean value of 0.28
506 approximately.

507
508 Taking into account these values, dense vegetation, in this study pasture, is found
509 from middle of October (interval 37) till the end of May (interval 19). It is in this period
510 where the precipitation concentrates (see Table 1). During the summer, the NDVI mean
511 values are lower than 0.3 corresponding with low precipitation and high temperatures.

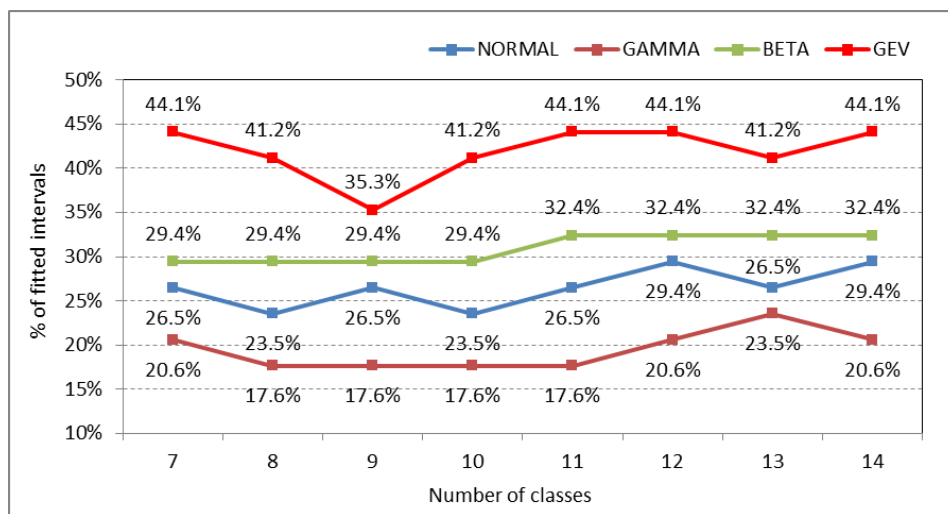
512
513 Following the work of Escribano-Rodriguez et al. (2014), there is a relationship of
514 pasture damage and a NDVI value around 0.40. Even if the authors point out that this
515 value is highly variable depending on the location, we can see that summer season in this
516 case study is under this value (see Fig. 4). This can explain that “Insurances for Damaged
517 Pasture” usually do not apply in these dates due to the arid environment (BOE, 2013).

518
519 MLM has been applied to model these 46 RV. Parameters have been calculated for 4
520 PDF (see Table 2) which are the candidates to be the best fit. To check the goodness of the

521 fit of PDF candidates, Chi square test (χ^2 test) has been used from 7 classes to 14 classes
 522 meeting the requirement that each class has at least five observations. The level of
 523 significance (α) was fixed to 5% for all the candidates.

524

525 Twelve intervals (from 23 to 34) corresponding to months of July, August and
 526 September have been excluded of this analysis since these intervals fall into the dry
 527 season in the study area, normally not cover by any SIBI. Therefore, calculations were
 528 carried out over 34 intervals. Fig. 5 shows the percentage of intervals that fit for every PDF
 529 candidate. The number of classes used in χ^2 test is represented at X-axis (from 7 to 14
 530 classes).



531

532 **Figure 5.** Percentage of fitted intervals (Y axis) for each PDF candidate (Normal, Gamma, Beta and
 533 GEV distributions) in function of the number of classes (X axis).

534

535 Fig. 5 indicates that GEV distributions explain more intervals (more than 40% for the
 536 majority of the class analysis) than Normal, Gamma or Beta distributions. An important
 537 difference between the Normal distribution and the rest of the PDF used in this work is its
 538 symmetry and kurtosis. Many of the observed NDVI distributions present a clear
 539 asymmetry and long tails in one or both sides that causes Normal distribution not to be
 540 the optimal fit.

541

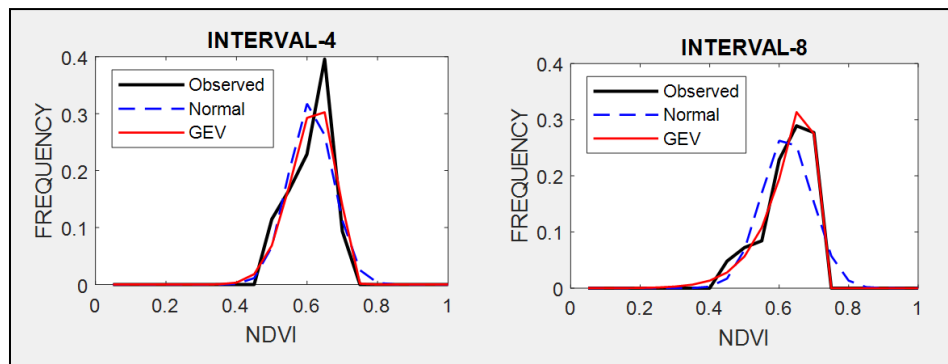
542 There is a relationship between seasons and the number of intervals that fit correctly.
 543 We found that GEV distributions explain better some intervals of spring and autumn since
 544 their observed distributions are very asymmetric. On the other hand, we did not find an
 545 important difference in winter, since its observed distributions are mainly symmetric.

546 Therefore, the methodology using the NDVI Normal assumption applied to design an
547 index-based insurance will not be feasible in many intervals of this study.

548

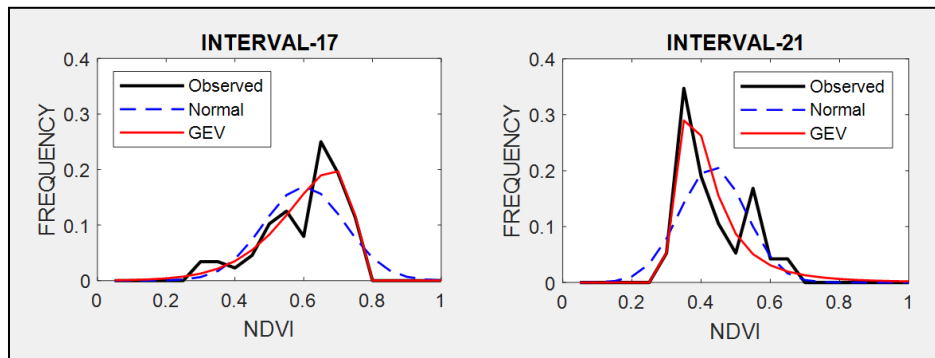
549 Table A1 at Appendix A shows the estimated parameters for each PDF and each
550 interval calculated by the MLM. These parameters were used to compare the estimated
551 PDF with the NDVI observed values on different times through the seasons. The following
552 intervals are shown as examples of better GEV fit: interval 4 and 8 (for winter, see Fig. 6),
553 interval 17 and 21 (for spring, see Fig. 7) and interval 36 and 40 (for autumn, see Fig. 8). In
554 these plots, observed frequency is compared versus Normal and GEV density distributions
555 calculated by MLM.

556



557

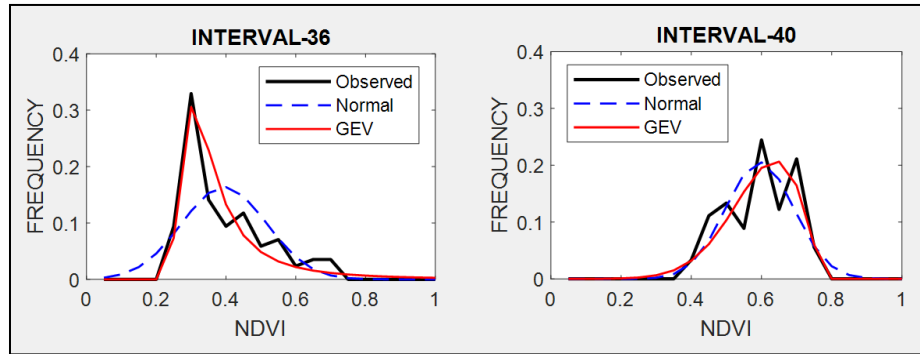
558 **Figure 6.** Comparison between observed NDVI frequency, GEV and Normal probability density
559 functions (PDF) on two different dates. Intervals 4 and 8 are examples for winter.



560

561 **Figure 7.** Comparison between observed NDVI frequency, GEV and Normal probability density
562 functions (PDF) on two different dates. Intervals 17 and 21 are examples for spring.

563



564

565 **Figure 8.** Comparison between observed NDVI frequency, GEV and Normal probability density
 566 functions (PDF) on two different times. Intervals 36 and 41 are examples for autumn.

567 During winter (see Fig. 6) the observed NDVI distribution presents negative skewness.
 568 Then, there is a higher frequency of high NDVI values corresponding with significant
 569 precipitation. During spring an evolution in the skewness is observed passing from
 570 negative to positive, and so, the lower NDVI values become the higher probable. Finally,
 571 during autumn precipitation begins and from positive pass to negative skewness and
 572 higher NDVI values are possible. We can observe that Normal distribution has no flexibility
 573 to follow this dynamic in the distributions on each time. This comparison is done in a
 574 sequential order for the whole of intervals in Figures A1, A2, A3 and A4 at Appendix A.

575

576 The more skewness and kurtosis depart from those of the Normal distribution the
 577 larger the errors affecting the insurance designed based on (Turvey et al., 2012). It is an
 578 expected result as pasture scenario is quite different from the development of a crop,
 579 where Normal distributions in the NDVI values are more expected. This high heterogeneity
 580 in time and space of NDVI estimated on pasture has been pointed out in several works
 581 (Martin-Sotoca et al, 2018). At the same time, more different is the observed NDVI
 582 frequency from a Normal distribution less representative is the average, and so, the
 583 median becomes a more representative value.

584

585 **3.3 Insurance context**

586 The use of NDVI thresholds in damaged pasture context was presented in the
 587 introduction section, being an example of using the "Insurance for Damaged Pasture" in
 588 Spain. We have chosen this last insurance to compare the results between applying
 589 Normal and GEV distribution methodologies. In this particular case the NDVI threshold
 590 ($NDVI_{th}$) was calculated using the expression $NDVI_{th} = \mu - k \cdot \sigma$ (where μ, σ are average and
 591 standard deviation of NDVI distributions respectively, assuming the Normal hypothesis).

592

593 The probability of being below $NDVI_{th}$ (using $k = 0.7$, first damage level in the
 594 insurance) at every interval has been calculated assuming the Normal hypothesis. As it
 595 was expected, this value is always 24.2% (see third column in Table 4). The probability of
 596 being below $NDVI_{th}$ has also been calculated using GEV distributions obtained in this
 597 study. The probability obtained by GEV distributions is mostly lower than the Normal
 598 distributions in spring, autumn and winter (see Table 4) that is the working period of the
 599 insurance.

600

601 Observing where in time are localized the highest relative error in probabilities (fifth
 602 column in Table 4), in absolute values, intervals corresponding to the end of winter,
 603 second middle of spring and the beginning of autumn present errors higher than 10%. This
 604 could explain why it is in spring and autumn when more disagreements exist between
 605 farmers and insurance company in claims.

606

607 **Table 4 – First column:** time intervals of approximately 8 days along the year. **Second column:** NDVI
 608 thresholds ($NDVI_{th}$) based on a Normal distribution applying $\mu - 0.7 \times \sigma$. **Third column:** percentages of
 609 area below the $NDVI_{th}$ when Normal distributions are applied. **Fourth column:** percentages of area
 610 below the $NDVI_{th}$ when GEV distributions are applied. **Fifth column:** relative area error of GEV
 611 compared to the Normal distribution.

612

| RANDOM VARIABLE | NORMAL | | GEV | |
|-----------------|-------------|--------|--------|-----------|
| | $NDVI_{th}$ | Prob. | Prob. | Error (%) |
| Interval 1 | 0.535 | 24.20% | 24.37% | 0.70% |
| Interval 2 | 0.541 | 24.20% | 23.18% | -4.21% |
| Interval 3 | 0.541 | 24.20% | 23.27% | -3.84% |
| Interval 4 | 0.543 | 24.20% | 23.27% | -3.84% |
| Interval 5 | 0.545 | 24.20% | 24.17% | -0.12% |
| Interval 6 | 0.534 | 24.20% | 21.48% | -11.24% |
| Interval 7 | 0.528 | 24.20% | 24.01% | -0.79% |
| Interval 8 | 0.546 | 24.20% | 20.70% | -14.46% |
| Interval 9 | 0.555 | 24.20% | 21.30% | -11.98% |
| Interval 10 | 0.561 | 24.20% | 22.28% | -7.93% |
| Interval 11 | 0.567 | 24.20% | 23.49% | -2.93% |
| Interval 12 | 0.572 | 24.20% | 23.75% | -1.86% |
| Interval 13 | 0.571 | 24.20% | 23.20% | -4.13% |
| Interval 14 | 0.570 | 24.20% | 24.29% | 0.37% |
| Interval 15 | 0.571 | 24.20% | 23.47% | -3.02% |

| | | | | |
|--------------------|-------|--------|--------|---------|
| Interval 16 | 0.560 | 24.20% | 23.26% | -3.88% |
| Interval 17 | 0.495 | 24.20% | 21.29% | -12.02% |
| Interval 18 | 0.484 | 24.20% | 21.58% | -10.83% |
| Interval 19 | 0.442 | 24.20% | 23.06% | -4.71% |
| Interval 20 | 0.381 | 24.20% | 27.20% | 12.40% |
| Interval 21 | 0.342 | 24.20% | 29.46% | 21.74% |
| Interval 22 | 0.323 | 24.20% | 28.84% | 19.17% |
| Interval 35 | 0.257 | 24.20% | 18.98% | -21.57% |
| Interval 36 | 0.285 | 24.20% | 28.57% | 18.06% |
| Interval 37 | 0.333 | 24.20% | 25.90% | 7.02% |
| Interval 38 | 0.398 | 24.20% | 24.27% | 0.29% |
| Interval 39 | 0.454 | 24.20% | 23.79% | -1.69% |
| Interval 40 | 0.503 | 24.20% | 22.81% | -5.74% |
| Interval 41 | 0.491 | 24.20% | 23.23% | -4.01% |
| Interval 42 | 0.517 | 24.20% | 24.66% | 1.90% |
| Interval 43 | 0.507 | 24.20% | 23.13% | -4.42% |
| Interval 44 | 0.514 | 24.20% | 23.49% | -2.93% |
| Interval 45 | 0.515 | 24.20% | 23.70% | -2.07% |
| Interval 46 | 0.509 | 24.20% | 23.33% | -3.60% |

613

614 In Table 4, Normal $NDVI_{th}$ have been used to calculate the probability in GEV distributions.
615 An alternative calculation can be the use of Normal probability (24.2%) to calculate new
616 $NDVI_{th}$ based on GEV (see Table 5). It can be seen that new $NDVI_{th}$ obtained by GEV
617 distributions are mostly upper than thresholds using Normal distributions in spring,
618 autumn and winter. Considering these results we find that damage thresholds calculated
619 by GEV methodology are mostly above that one's calculated by Normal methodology.

620 Again, intervals corresponding to the end of winter, second middle of spring and the
621 beginning of autumn present $NDVI_{th}$ relative errors higher than 1% in absolute values
622 (fourth column in Table 5).

623

624 **Table 5 - First column:** time intervals of approximately 8 days along the year. **Second column:** NDVI
625 thresholds ($NDVI_{Th}$) based on a Normal distribution (Normal) applying $\mu - 0.7 \times \sigma$. **Third column:**
626 $NDVI_{Th}$ based on a GEV distribution (GEV) using 24.2% as the area below the $NDVI_{Th}$. **Fourth column:**
627 relative $NDVI_{Th}$ error of GEV compared to the Normal distribution.

628

| RANDOM VARIABLE | NDVI _{Th} | | Error (%) |
|-----------------|--------------------|-------|-----------|
| | Normal | GEV | |
| Interval 1 | 0.535 | 0.534 | -0,19% |
| Interval 2 | 0.541 | 0.543 | 0,37% |
| Interval 3 | 0.541 | 0.543 | 0,37% |
| Interval 4 | 0.543 | 0.545 | 0,37% |
| Interval 5 | 0.545 | 0.545 | 0,00% |
| Interval 6 | 0.534 | 0.543 | 1,69% |
| Interval 7 | 0.528 | 0.528 | 0,00% |
| Interval 8 | 0.546 | 0.558 | 2,20% |
| Interval 9 | 0.555 | 0.563 | 1,44% |
| Interval 10 | 0.561 | 0.567 | 1,07% |
| Interval 11 | 0.567 | 0.569 | 0,35% |
| Interval 12 | 0.572 | 0.574 | 0,35% |
| Interval 13 | 0.571 | 0.574 | 0,53% |
| Interval 14 | 0.570 | 0.569 | -0,18% |
| Interval 15 | 0.571 | 0.573 | 0,35% |
| Interval 16 | 0.560 | 0.563 | 0,54% |
| Interval 17 | 0.495 | 0.510 | 3,03% |
| Interval 18 | 0.484 | 0.498 | 2,89% |
| Interval 19 | 0.442 | 0.447 | 1,13% |
| Interval 20 | 0.381 | 0.374 | -1,84% |
| Interval 21 | 0.342 | 0.334 | -2,34% |
| Interval 22 | 0.323 | 0.318 | -1,55% |
| Interval 35 | 0.257 | 0.262 | 1,95% |
| Interval 36 | 0.285 | 0.278 | -2,46% |
| Interval 37 | 0.333 | 0.327 | -1,80% |
| Interval 38 | 0.398 | 0.398 | 0,00% |
| Interval 39 | 0.454 | 0.455 | 0,22% |
| Interval 40 | 0.503 | 0.508 | 0,99% |
| Interval 41 | 0.491 | 0.494 | 0,61% |
| Interval 42 | 0.517 | 0.516 | -0,19% |
| Interval 43 | 0.507 | 0.510 | 0,59% |
| Interval 44 | 0.514 | 0.516 | 0,39% |
| Interval 45 | 0.515 | 0.516 | 0,19% |
| Interval 46 | 0.509 | 0.511 | 0,39% |

629

630

631 **4. Conclusions**

632 According to the results obtained in the study area using MLM and χ^2 test, it can be
633 concluded that Normal distributions are not the best fit to the NDVI observations, and
634 GEV distributions provide a better approximation.

635

636 The difference between Normal and GEV assumption is more evident in the transition
637 from winter to summer (spring), where NDVI values decrease, and then from summer to
638 winter (autumn) presenting the opposite behavior of increasing NDVI values. In both
639 periods asymmetrical distributions were found, negative skewness for the spring
640 transition and positive skewness for the autumn transition. During both periods the
641 variability in precipitation and temperatures were higher in this location.

642

643 We have found differences if GEV assumption is selected instead of the Normal one
644 when defining damaged pasture thresholds ($NDVI_{th}$). The use of these different
645 assumptions should be taken into account in future insurance implementations due to the
646 important consequences of supposing a damage event or not. We propose the use of
647 **quantiles** in observed NDVI distributions instead of average and standard deviation,
648 typically of Normal distributions, to calculate new $NDVI_{th}$.

649

650

651

652

653 **Acknowledgements**

654 This research has been partially supported by funding from MINECO under contract No.
655 MTM2015-63914-P and CICYT PCIN-2014-080.

656

657 **Appendix A**

658

659

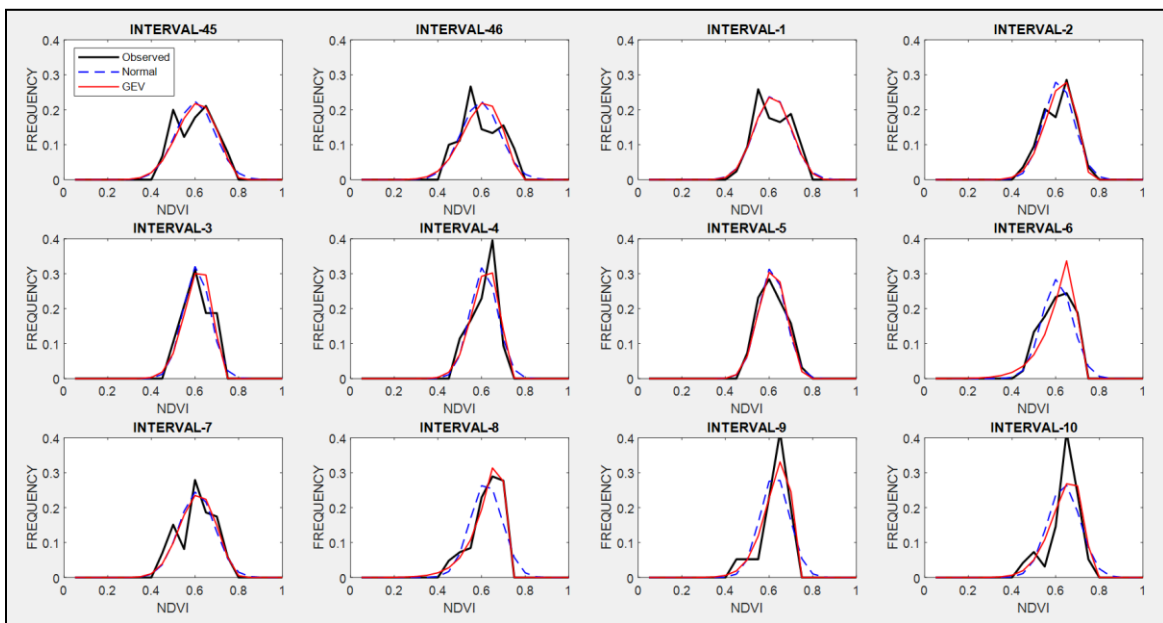
Table A1 - Maximum Likelihood parameters calculated for 4 PDF.

| RANDOM VARIABLE | NORMAL | | GAMMA | | BETA | | GEV | | |
|-----------------|--------|----------|----------|---------|--------|--------|-------|----------|--------|
| | μ | σ | α | β | a | b | μ | σ | ξ |
| Interval 1 | 0.591 | 0.081 | 53.31 | 0.011 | 21.45 | 14.82 | 0.563 | 0.080 | -0.297 |
| Interval 2 | 0.589 | 0.069 | 71.14 | 0.008 | 30.62 | 21.40 | 0.571 | 0.073 | -0.477 |
| Interval 3 | 0.583 | 0.060 | 94.15 | 0.006 | 39.56 | 28.34 | 0.567 | 0.063 | -0.457 |
| Interval 4 | 0.585 | 0.060 | 91.88 | 0.006 | 39.58 | 28.05 | 0.570 | 0.064 | -0.468 |
| Interval 5 | 0.588 | 0.061 | 93.92 | 0.006 | 38.83 | 27.25 | 0.568 | 0.061 | -0.340 |
| Interval 6 | 0.582 | 0.068 | 70.28 | 0.008 | 30.67 | 22.05 | 0.577 | 0.083 | -0.846 |
| Interval 7 | 0.584 | 0.080 | 52.52 | 0.011 | 22.16 | 15.82 | 0.559 | 0.082 | -0.366 |
| Interval 8 | 0.596 | 0.071 | 65.37 | 0.009 | 28.89 | 19.59 | 0.591 | 0.081 | -0.833 |
| Interval 9 | 0.601 | 0.066 | 76.02 | 0.008 | 34.31 | 22.84 | 0.590 | 0.070 | -0.652 |
| Interval 10 | 0.613 | 0.073 | 63.83 | 0.010 | 27.80 | 17.62 | 0.598 | 0.079 | -0.572 |
| Interval 11 | 0.621 | 0.078 | 58.72 | 0.011 | 24.33 | 14.86 | 0.600 | 0.083 | -0.451 |
| Interval 12 | 0.624 | 0.073 | 68.33 | 0.009 | 28.01 | 16.94 | 0.603 | 0.078 | -0.431 |
| Interval 13 | 0.624 | 0.075 | 66.22 | 0.009 | 26.23 | 15.85 | 0.604 | 0.080 | -0.476 |
| Interval 14 | 0.631 | 0.088 | 50.23 | 0.013 | 18.71 | 10.92 | 0.603 | 0.090 | -0.342 |
| Interval 15 | 0.630 | 0.084 | 53.60 | 0.012 | 21.17 | 12.45 | 0.607 | 0.089 | -0.448 |
| Interval 16 | 0.627 | 0.096 | 38.75 | 0.016 | 16.08 | 9.59 | 0.602 | 0.103 | -0.474 |
| Interval 17 | 0.577 | 0.117 | 20.47 | 0.028 | 10.24 | 7.58 | 0.560 | 0.127 | -0.692 |
| Interval 18 | 0.568 | 0.120 | 20.52 | 0.028 | 9.71 | 7.42 | 0.552 | 0.136 | -0.718 |
| Interval 19 | 0.523 | 0.116 | 19.46 | 0.027 | 9.52 | 8.68 | 0.495 | 0.125 | -0.493 |
| Interval 20 | 0.452 | 0.101 | 20.99 | 0.022 | 10.98 | 13.31 | 0.401 | 0.077 | 0.078 |
| Interval 21 | 0.409 | 0.095 | 19.94 | 0.021 | 11.18 | 16.13 | 0.354 | 0.060 | 0.325 |
| Interval 22 | 0.379 | 0.080 | 24.66 | 0.015 | 14.41 | 23.52 | 0.333 | 0.046 | 0.385 |
| Interval 23 | 0.353 | 0.073 | 26.54 | 0.013 | 15.85 | 29.01 | 0.311 | 0.036 | 0.456 |
| Interval 24 | 0.328 | 0.056 | 38.36 | 0.009 | 24.22 | 49.65 | 0.298 | 0.033 | 0.287 |
| Interval 25 | 0.305 | 0.044 | 53.52 | 0.006 | 35.62 | 81.20 | 0.282 | 0.028 | 0.210 |
| Interval 26 | 0.298 | 0.034 | 78.93 | 0.004 | 54.47 | 128.55 | 0.283 | 0.029 | -0.064 |
| Interval 27 | 0.289 | 0.026 | 126.85 | 0.002 | 88.33 | 217.15 | 0.278 | 0.021 | -0.030 |
| Interval 28 | 0.282 | 0.022 | 166.17 | 0.002 | 119.50 | 305.03 | 0.274 | 0.022 | -0.322 |
| Interval 29 | 0.278 | 0.021 | 179.09 | 0.002 | 127.93 | 332.63 | 0.269 | 0.018 | -0.085 |
| Interval 30 | 0.273 | 0.019 | 203.11 | 0.001 | 147.67 | 393.21 | 0.266 | 0.019 | -0.247 |
| Interval 31 | 0.272 | 0.022 | 166.83 | 0.002 | 120.11 | 321.95 | 0.262 | 0.018 | -0.059 |
| Interval 32 | 0.280 | 0.034 | 75.63 | 0.004 | 52.36 | 134.30 | 0.264 | 0.023 | 0.118 |
| Interval 33 | 0.285 | 0.034 | 82.05 | 0.004 | 54.90 | 137.68 | 0.270 | 0.020 | 0.122 |
| Interval 34 | 0.295 | 0.057 | 33.26 | 0.009 | 21.15 | 50.37 | 0.268 | 0.024 | 0.363 |

| | | | | | | | | | |
|--------------------|-------|-------|-------|-------|-------|-------|-------|-------|--------|
| Interval 35 | 0.312 | 0.079 | 19.70 | 0.016 | 11.83 | 25.94 | 0.275 | 0.038 | 0.300 |
| Interval 36 | 0.369 | 0.121 | 10.81 | 0.034 | 6.11 | 10.33 | 0.298 | 0.063 | 0.480 |
| Interval 37 | 0.432 | 0.141 | 9.45 | 0.046 | 5.21 | 6.81 | 0.370 | 0.120 | -0.080 |
| Interval 38 | 0.487 | 0.128 | 13.88 | 0.035 | 7.25 | 7.63 | 0.445 | 0.127 | -0.321 |
| Interval 39 | 0.529 | 0.107 | 23.56 | 0.022 | 11.39 | 10.16 | 0.497 | 0.110 | -0.390 |
| Interval 40 | 0.570 | 0.096 | 34.02 | 0.017 | 15.10 | 11.40 | 0.548 | 0.105 | -0.533 |
| Interval 41 | 0.554 | 0.090 | 36.42 | 0.015 | 16.90 | 13.64 | 0.531 | 0.096 | -0.471 |
| Interval 42 | 0.583 | 0.095 | 37.29 | 0.016 | 15.56 | 11.11 | 0.551 | 0.094 | -0.295 |
| Interval 43 | 0.574 | 0.097 | 34.27 | 0.017 | 14.93 | 11.07 | 0.550 | 0.103 | -0.482 |
| Interval 44 | 0.572 | 0.083 | 47.13 | 0.012 | 20.40 | 15.26 | 0.549 | 0.086 | -0.425 |
| Interval 45 | 0.576 | 0.088 | 42.59 | 0.014 | 18.17 | 13.36 | 0.550 | 0.090 | -0.396 |
| Interval 46 | 0.570 | 0.088 | 41.98 | 0.014 | 18.11 | 13.66 | 0.546 | 0.092 | -0.445 |

660

661



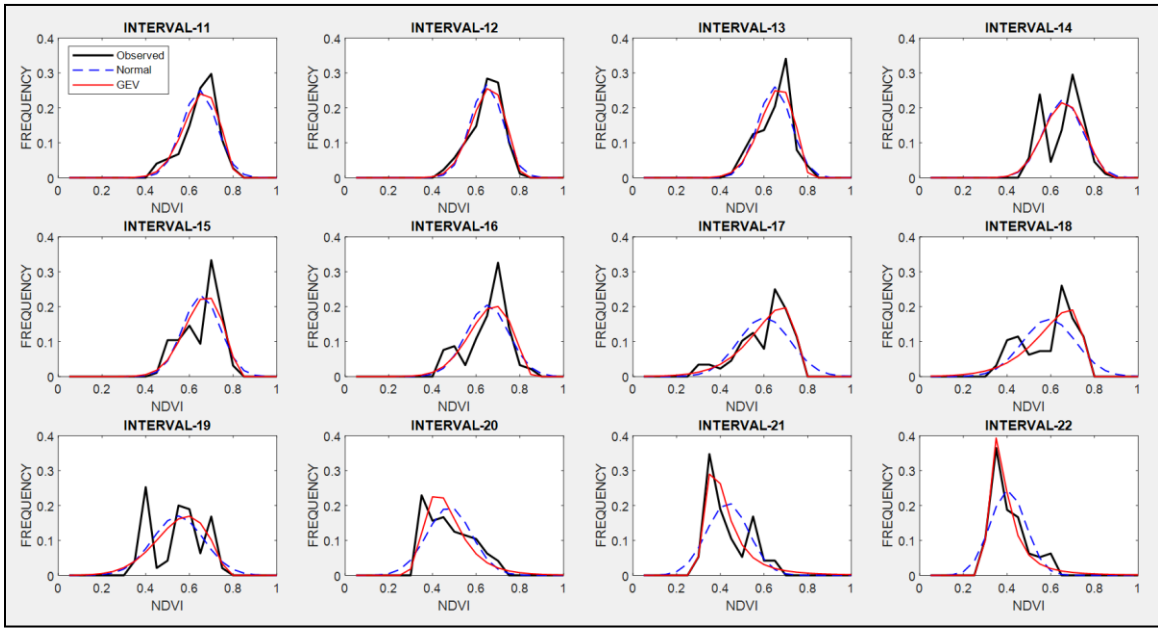
662

663

664

Figure A1. Observed NDVI, GEV and Normal probability density functions (PDF) from interval 45 to interval 10 (from 19 December to 21 March) representing winter.

665



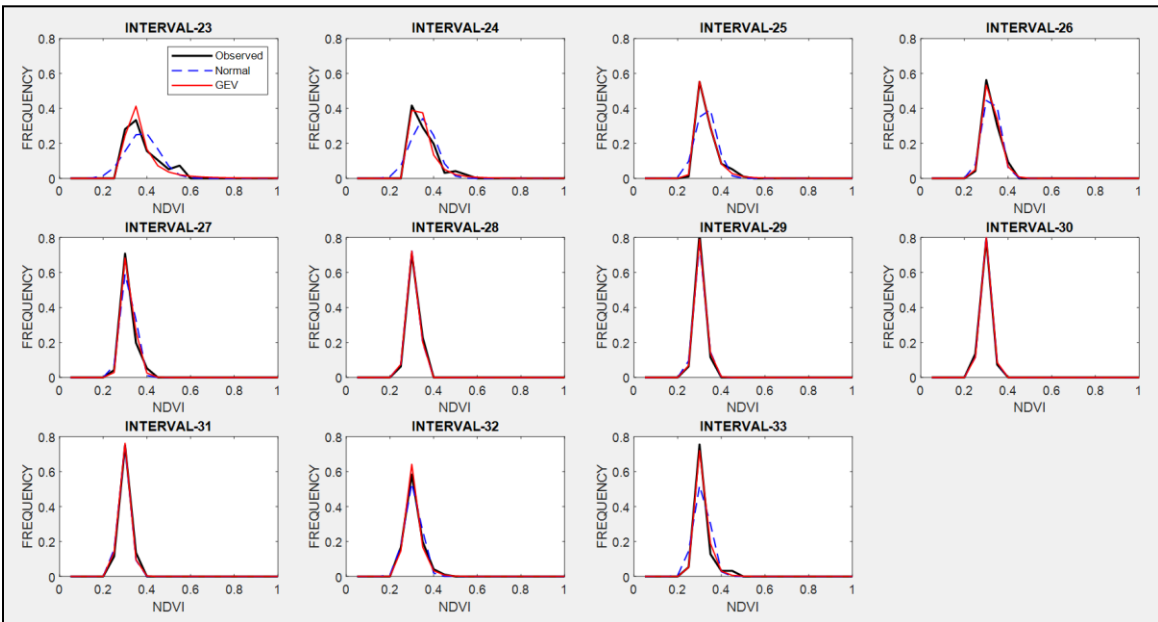
666

667

668

Figure A2. Observed NDVI, GEV and Normal probability density functions (PDF) from interval 11 to interval 22 (from 22 March to 25 June) representing spring.

669



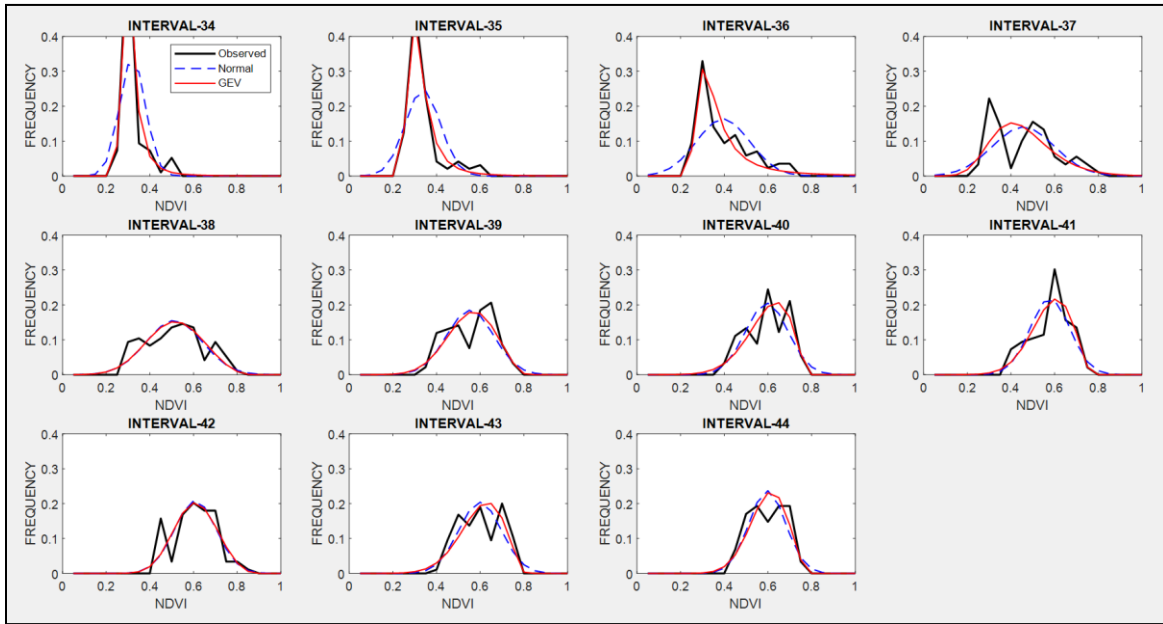
670

671

672

Figure A3. Observed NDVI, GEV and Normal probability density functions (PDFs) from interval 23 to interval 33 (from 26 June to 21 September) representing summer.

673



674

675

676

Figure A4. Observed NDVI, GEV and Normal PDFs from interval 34 to interval 44 (from 22 September to 18 December) representing autumn.

677

678 **References**

679

680 Agencia Estatal de Meteorología (AEMET). Available at: www.aemet.es, 2017.

681 Al-Bakri, J. T., and Taylor, J. C.: Application of NOAA AVHRR for monitoring vegetation
682 conditions and biomass in Jordan, *J. Arid Environ*, 54, 579–593, 2003.

683 Bailey, S.: The Impact of Cash Transfers on Food Consumption in Humanitarian Settings: A
684 review of evidence, Study for the Canadian Foodgrains Bank, May 2013.

685 Boletín Oficial del Estado (BOE, 6638 - Orden AAA/1129/2013. Nº 145, III, p-46077, 2013.

686 Cochran, William G.: The Chi-square Test of Goodness of Fit, *Annals of Mathematical
687 Statistics*. 23: 315–345, 1952.

688 Crimmins, M. A., and Crimmins T. M.: Monitoring plant phenology using digital repeat
689 photography, *Environ. Manage*, 41, 949-958, 2008.

690 Dalezios, N. R., Blanta, A., Spyropoulos, N. V., and Tarquis A. M.: Risk identification of
691 agricultural drought for sustainable Agroecosystems, *Nat. Hazards Earth Syst. Sci.*, 14,
692 2435–2448, 2014.

693 Dalezios, N. R.: The Role of Remotely Sensed Vegetation Indices in Contemporary
694 Agrometeorology. Invited paper in Honorary Special Volume in memory of late Prof. A.
695 Flokas. Publisher: Hellenic Meteorological Association, 33-44, 2013.

696 De Leeuw, J., Vrieling, A., Shee, A., Atzberger, C., Hadgu, K. M., Biradar, C. M., Humphrey
697 Keah, H., and Turvey, C.: The Potential and Uptake of Remote Sensing in Insurance: A
698 Review, *Remote Sens.*, 6(11), 10888-10912, 2014.

699 Escribano Rodríguez, J. Agustín, Díaz-Ambrona, Carlos Gregorio H., and Tarquis Alfonso,
700 Ana María: Selection of vegetation indices to estimate pasture production in Dehesas,
701 *PASTOS*, 44(2), 6-18, 2014.

702 Fensholt, R., and Proud, S. R.: Evaluation of earth observation based global long term
703 vegetation trends - comparing GIMMS and MODIS global NDVI time series, *Remote
704 Sens. Environ.*, 119, 131–147, 2012.

705 Flynn E. S.: Using NDVI as a pasture management tool. Master Thesis, University of
706 Kentucky, 2006.

707 Forkel, M., Carvalhais, N., Verbesselt, J., Mahecha, M.D., Neigh, C. S., and Reichstein, M.:
708 Trend change detection in NDVI time series: effects of inter-annual variability and
709 methodology, *Remote Sens.*, 5, pp, 2113–2144, 2013.

710 Fuller, D.O.: Trends in NDVI time series and their relation to rangeland and crop production
711 in Senegal, 1987–1993, *Int. J. Remote Sens.*, 19, 2013–2018, 1998.

712 Gommès, R., and Kayitakire, F.: The challenges of index-based insurance for food security
713 in developing countries. Proceedings, Technical Workshop, JRC, Ispra, 2-3 May 2012.
714 Publisher: JRC-EC, p. 276, 2013.

715 Gouveia, C., Trigo, R. M., and Da Camara, C. C.: Drought and vegetation stress monitoring
716 in Portugal using satellite data, *Nat. Hazards Earth Syst. Sci.*, 9, 185-195, 2009.

717 Goward, S. N., Tucker, C. J., and Dye, D.G.: North-American vegetation patterns observed
718 with the NOAA-7 advanced very high-resolution radiometer. *Vegetation*, 64, 3–14,
719 1985.

720 Graham, E. A., Yuen, E. M., Robertson, G. F., Kaiser, W. J., Hamilton, M. P., and Rundel, P.
721 W.: Budburst and leaf area expansion measured with a novel mobile camera system
722 and simple color thresholding, *Environ. Exp. Bot.*, 65, 238-244, 2009.

723 Hobbs, T. J.: The use of NOAA-AVHRR NDVI data to assess herbage production in the arid
724 rangelands of central Australia, *Int. J. Remote Sens.*, 16, 1289–1302, 1995.

725 Holben, B. N.: Characteristics of maximum-value composite images from temporal AVHRR
726 data, *Int. J. Remote Sens.*, 7, 1417–1434, 1986.

727 Kottek, M., Grieser, J., Beck, C., Rudolf, B., and Rubel, F.: World Map of the Köppen-Geiger
728 climate classification updated, *Meteorologische Zeitschrift*, 15, 259-263, 2006.

729 Kundu, A., Dwivedi, S., and Dutta, D.: Monitoring the vegetation health over India during
730 contrasting monsoon years using satellite remote sensing indices, *Arab J Geosci.*, 9,
731 144, 2016.

732 Land Processes Distributed Active Archive Center (LP DAAC): Surface Reflectance 8-Day L3
733 Global 500m. NASA and USGS. Available at:
734 https://lpdaac.usgs.gov/products/modis_products_Table/mod09a1. 2014.

735 Larson, H. J.: *Introduction to Probability Theory and Statistical Inference* (3rd edition). New
736 York, John Wiley and Sons, 1982.

737 Leblois, A.: Weather index-based insurance in a cash crop regulated sector: ex ante
738 evaluation for cotton producers in Cameroon. Paper presented at the JRC/IRI
739 workshop on The Challenges of Index-Based Insurance for Food Security in Developing
740 Countries, Ispra, 2-3, May, 2012.

741 Lovejoy, S., Tarquis, A. M., Gaonac’h, H., and Schertzer, D.: Single and Multiscale remote
742 sensing techniques, multifractals and MODIS derived vegetation and soil moisture.
743 *Vadose Zone J.*, 7, 533-546, 2008.

744 Maples, J. G., Brorsen, B. W., and Biermachs, J. T.: The rainfall Index Annual Forage pilot
745 program as a risk management tool for cool-season forage. *J. Agr. Appl Econ*, 48(1),
746 29–51, 2016.

747 Martin-Sotoca, J. J., Saa-Requejo, A., Orondo J. B., and Tarquis, A. M.: Singularity maps
748 applied to a vegetation index. *Bio. Eng.* 168, 42-53, 2018.

749 Motohka, T., Nasahara, K. N., Murakami, K., and Nagai, S.: Evaluation of sub-pixel cloud
750 noises on MODIS daily spectral indices based on in situ measurements, *Remote Sens.*,
751 3, 1644–1662, 2011.

752 Niemeyer, S.: New drought indices, First Int. Conf. on Drought Management: Scientific and
753 Technological Innovations, Zaragoza, Spain. Joint Research Centre of the European
754 Commission, Available online at
755 <http://www.iamz.ciheam.org/medroplan/zaragoza2008/Sequia2008/Session3/S.Niemeyer.pdf>, 2008.
756

757 Ortega-Farias, S., Ortega-Salazar, S., Poblete, T., Kilic, A., Allen, R., Poblete-Echeverría, C.,
758 Ahumada-Orellana, L., Zuñiga, M., and Sepúlveda, D.: Estimation of Energy Balance
759 Components over a Drip-Irrigated Olive Orchard Using Thermal and Multispectral
760 Cameras Placed on a Helicopter-Based Unmanned Aerial Vehicle (UAV), *Remote Sens.*,
761 8, 638, pp 18, 2016.

762 Park, S.: Cloud and cloud shadow effects on the MODIS vegetation index composites of the
763 Korean Peninsula, *Int. J. Remote Sens.*, 34, 1234–1247, 2013.

764 Rao, K. N.: Index based Crop Insurance, *Agric. Agric. Sci. Proc.*, 1, 193–203, 2010.

765 Roumiguié, A., Sigel, G., Poilvé, H., Bouchard, B., Vrieling, A., and Jacquin, A.: Insuring
766 forage through satellites: testing alternative indices against grassland production
767 estimates for France, *Int. J. Remote Sens.*, 38, 1912-1939, 2017.

768 Roumiguié, A., Jacquin, A., Sigel, G., Poilvé, H., Lepoivre, B., and Hagolle, O.: Development
769 of an index-based insurance product: validation of a forage production index derived
770 from medium spatial resolution fCover time series, *GIScience Remote Sens.*, 52, 94-
771 113, 2015.

772 Tackenberg, Oliver: A New Method for Non-destructive Measurement of Biomass, Growth
773 Rates, Vertical Biomass Distribution and Dry Matter Content Based on Digital Image
774 Analysis, *Annals of Botany*, 99(4), 777–783, 2007.

775 Turvey, C. G., and Mcaurin, M. K.: Applicability of the Normalized Difference Vegetation
776 Index (NDVI) in Index-Based Crop Insurance Design, *Am. Meteorol. Soc.*, 4, 271-284,
777 2012.

778 UNEP Word Atlas of Desertification: Second Ed. United Nations Environment Programme,
779 Nairobi, 1997.

780 USDA. U.S. Department of Agriculture, Federal Crop Insurance Corporation, Risk
781 Management Agency: Rainfall Index Plan Annual Forage Crop Provisions. 16- RI-AF.
782 <http://www.rma.usda.gov/policies/ri-vi/2015/16riaf.pdf> 2013 (Accessed March 1,
783 2018).

784 Wei, W., Wu, W., Li, Z., Yang, P., and Qingbo Zhou, Q.: Selecting the Optimal NDVI Time-
785 Series Reconstruction Technique for Crop Phenology Detection, *Intell. Autom. Soft. Co.*
786 22, 237-247, 2016.
787
788
789
790